

# Proposed Subgradient-Based Solution for Coordination of Distributed Energy Resources in a Microgrid

V.Srinivasulu<sup>1</sup>, M Madhusudhan Reddy<sup>2</sup>

**Abstract**--This paper presents new proposed fully-distributed cooperative control for a microgrid to work autonomously with high renewable energy penetration. For a microgrid to work autonomously, it must maintain its own supply-demand balance in term of active power and regulate the system frequency and voltage magnitudes. As the Distributed Generators within a microgrid could be diverse and distributed, the control and management solutions should be as efficient and cost-effective as possible for the microgrid to be economically viable. Since well-designed distributed control solutions can be flexible, reliable, scalable, and low-cost to implement thus they are promising choice for the control and operation of microgrids. As the popular maximum peak power tracking (MPPT) algorithms emphasize high energy usage efficiency but may cause a supply-demand imbalance when the maximum available renewable generations are more than demanded, especially for autonomous micro-grids. To maintain supply and demand, energy storage devices are used, however its effectiveness is also limited. presently conventional droop control is one of the most popular decentralized methods for sharing active and reactive loads among the distributed generators. However this method have several drawbacks, such as voltage and frequency deviations, inaccurate power sharing, and unsatisfactory transient performances. To overcome these problems, this paper proposes a distributed subgradient-based solution to coordinate the operations of different types of distributed renewable generators in a microgrid. By controlling the utilization levels of renewable generators, the supply-demand balance can be well maintained and the system dynamic performance can be significantly improved. Simulation results demonstrate the effectiveness of the proposed control solution..

**Index Terms**— Distributed, co operative control , micro grid control, micro grid, multi agent system, renewable generator.



## I. INTRODUCTION

A micro grid can be defined as a cluster of loads, distributed generators (DGs) and energy storage systems that is serviced by a distribution network and can operate in both grid connected and islanded modes. The size of a micro grid may range from a typical housing estate, isolated rural communities, to mixed suburban environments, academic or public communities, to commercial areas, industrial sites and trading estates, or municipal regions. The benefits of micro grids include their increased reliability, improved energy efficiency, reduced environmental impact, and timely response to growing consumer demand. A micro grid is a quite appealing alternative for overcoming the challenges of integrating distributed energy resource units, including renewable energy sources, into power systems .

Wind and solar power are among the most promising renewable power supply alternatives due to their abundance, cleanness and low production cost/unit. However, the intermittency of wind and solar power poses new challenges to the operation and control of micro grids, especially under high penetration. One important issue is

the power reference control Of distributed renewable generators (RGs) under dynamic weather and load conditions. The popular maximum peak power tracking (MPPT) algorithms emphasize high energy usage efficiency but may cause a supply-demand imbalance when the maximum available renewable generations are more than demanded, especially for autonomous micro grids. To overcome this problem, energy storage devices such as batteries, super-capacitors and flywheels can be used to absorb the excess energy .However, if the installed energy storage device's capacity is still insufficient, the outputs of the renewable generators will have to be controlled to ensure the supply-demand balance. Even if sufficient energy storage devices are available, their effectiveness is limited by the maximum charging and discharging rate and charging level. For an autonomous micro grid, the control issues are very similar to those of large-scale power systems, such as supply-demand balance and frequency regulation. Due to the similarity, most existing ideas on traditional power system operation can be introduced to small scale autonomous micro grids.

In, the authors propose a two-level control scheme for a wind farm, which consists of supervisory and machine levels of control. In this scheme, the supervisory control level decides the active and reactive power set points for all doubly-fed induction generators (DFIGs), while the machine control level ensures that the set points are reached. In the authors propose an optimal dispatch control strategy for a wind farm. The DFIGs were controlled to adjust the active and reactive power generation according to the request of the system's central operator. In the authors present a control approach for a wind farm to provide a sufficient generating margin upon the request of supervisory controllers. In the authors present a coordinated control method for leveling photovoltaic (PV) generation. This control scheme uses fuzzy reasoning to generate the central leveling generation commands to reduce the frequency deviation of the isolated power utility. All of these methods are centralized, therefore requiring complicated communication networks to collect information globally and a powerful central controller to process huge amounts of data. Thus, these solutions are costly to implement and susceptible to single-point failures. Due to the intermittency of renewable generation, more frequent control updates are required. The centralized solutions may not be able to respond in a timely fashion if operating conditions change rapidly and unexpectedly.

This paper targets small-scale, self-contained, medium voltage micro grid power systems, which are composed of multiple RGs, a reliable synchronous generator (SG), and loads. For a micro grid to work autonomously, it must maintain its own supply-demand balance in term of active power and regulate the system frequency and voltage magnitudes. As the DGs within a micro grid could be diverse and distributed, the control and management solutions should be as efficient and cost-effective as possible for the micro grid to be economically viable. Since well-designed distributed control solutions can be flexible, reliable, scalable, and low-cost to implement, thus they are promising choice for the control and operation of micro grids. Multi-agent system (MAS) is one of the most popular distributed

Control approaches in literature. The concept of MAS has been wide applied to various problems in micro grid research, such as power management, distributed optimization, active power and reactive power control.

Existing MAS based applications in power systems are usually rule-based and lacked rigorous stability analysis. Recent developments in consensus and cooperative control have been successfully applied, that can improve the stability and applicability of MAS-based solutions. According to the MAS-based fully-distributed control solution presented in this paper, each RG controller has two control levels. The upper control level implements a sub gradient based optimization algorithm, which can maintain the supply-demand balance by adjusting local utilization levels of RGs based on local frequency measurement and maximum renewable power prediction. Once the utilization level is updated, the reference for local active power generation of the RGs can be calculated and deployed by the lower control level.

The DGs can be controlled either in voltage regulation mode or in reactive power control mode. The control settings for different control modes can be decided locally according to operating conditions. In this paper, the coordination of multiple RGs in a micro grid is formulated as a convex optimization problem that can be solved using the distributed sub gradient algorithm introduced. By adopting the near-optimal and stable coefficients setting algorithm introduced, the convergence of the fully distributed MAS-based algorithm can be guaranteed. In addition, only local frequency measurement, predicted maximum generation, and neighboring generators' utilization levels are needed to update local utilization level, which is realized by designing a control law based on the models of frequency dynamics introduced. The rest of the paper is organized as follows. Section II briefly introduces conventional droop control. Section III describes the proposed control approach. Section IV introduces the machine level control design. Section V presents simulation results with the 6-busmicrogrid. Finally, Section VI provides the conclusion and suggestions for future work.

## II. CONVENTIONAL DROOP CONTROL:

A micro grid can operate in either grid-connected mode or islanded mode. In grid-connected mode, the micro grid can either inject power into, or absorb power from, the main grid. The supply-demand can be assumed to be balanced by the main grid most of the time. In this scenario, each RG is controlled simply to operate under the MPPT method. However, when a micro grid operates in

islanded mode, the supply-demand should be balanced autonomously. Therefore, each component in the micro grid should cooperate to achieve this goal. Droop control methods, which originate from the principle of power balance of synchronous generators in large interconnected power systems, are proposed to ensure good power sharing for a power grid. For convenience, the conventional droop control method is briefly introduced as follows. To maintain the frequency of an autonomous micro grid, the active power outputs of each RG must be adjusted according to predefined droop characteristics as

$$P_i = P_i^0 + kf_{,i}(f^* - f_i) \tag{1}$$

where  $P_i^0$  and  $f_i^0$  are the rated operating and locally-measured frequency of the micro grid, respectively;  $k$  is the frequency droop coefficient for RG  $i$ ;  $P_i^0$  is the initial active power generation corresponding to  $f_i^0$ ; and  $P_i$  is the updated active power generation demand of RG  $i$ . In a similar manner, the reactive power of each RG can be adjusted according to the predefined droop characteristics as

$$Q_i = Q_i^0 + kv_{,i}(V^* - V_i) \tag{2}$$

where  $V_i^0$  and  $Q_i^0$  are the rated and measured voltage magnitudes, respectively;  $k$  is the voltage droop coefficient for RG  $i$ ;  $Q_i^0$  is the initial reactive power generation corresponding to  $V_i^0$ ; and  $Q_i$  is the output reactive power reference of RG  $i$ . The primary advantage of droop control is that it does not require direct communication between DER units. However, conventional droop controllers have several drawbacks, such as voltage and frequency deviations, inaccurate power sharing, and unsatisfactory transient performances, as summarized. To overcome the problems with droop control, mainly the frequency deviation, automatic generation control (AGC) can be applied to adjust the generation references periodically.

### III. PROPOSED SUBGRADIENT-BASED SOLUTION:

This section introduces the proposed fully-distributed algorithm, which can achieve the system's power supply-demand balance within the micro grid.

#### Utilization Level Based Coordination

The total active power demand calculated as of a microgrid can be

$$P_D = \sum_{i=1}^n P_{L,i} + P_{Loss} \tag{3}$$

Where  $n$  is the number of buses in the microgrid,  $P_{L,i}$  is the demand of load at bus  $i$ , and  $P_{Loss}$  is the active power loss in the microgrid.

The total available renewable power generation in the micro-grid can be calculated as

$$P_G^{max} = \sum_{i=1}^m P_{G,i}^{max} \tag{4}$$

Where  $m$  is the number of RGs, and  $P_{G,i}^{max}$  is the maximum power generation of RG  $i$ .

In an autonomous microgrid, if  $P_G^{max}$  is less than  $P_D$ , all RGs will operate in MPPT mode, and the SG(s) should compensate the generation deficiency. On the other hand, if  $P_G^{max}$  is larger than  $P_D$ , MPPT control strategies no longer apply. A suitable deloading strategy is required to share the load demands among the RGs, which can be accomplished by controlling the utilization levels ( $u_i$ s) of RGs to a common value

$$u^* = \min \left\{ \frac{P_D}{P_G^{max}}, 1 \right\} \tag{5}$$

Where  $u^*$  is the common utilization level for all RGs.

The active power generation reference  $P_{G,i}^{ref}$  of RG  $i$  is calculated as

$$P_{G,i}^{ref} = u^* \cdot P_{G,i}^{max} \tag{6}$$

According to (4) and (6), it can be easily verified that the supply-demand balance can be guaranteed when the maximum available renewable generation exceeds the load demand, as

$$\sum_{i=1}^m P_{G,i}^{ref} = \sum_{i=1}^m u^* \cdot P_{G,i}^{max} = \frac{P_D}{P_G^{max}} \sum_{i=1}^m P_{G,i}^{max} = P_D \tag{7}$$

#### 2.2 Distributed Generation Coordination Algorithm

In an autonomous microgrid, to ensure static stability, the supply and demand balance must be maintained. The objective for multiple RGs coordination is to minimize the function formulated as

$$\text{Min } H(u_i[k]) = \frac{1}{2} \left( \sum_{i=1}^m u_i[k] P_{G,i}^{max} - P_D \right)^2 \tag{8}$$

Where  $k$  is the discrete time step,  $u_i[k]$  is the utilization level of RG  $i$  at step  $k$ .

This convex optimization problem can be solved using distributed subgradient algorithm. According to [21]-[23],  $u_i[k]$  can be updated according

$$u_i[k+1] = \sum_{j=1}^m a_{ij} u_j[k] - d_i \frac{\partial H(u_i[k])}{\partial u_i[k]} \tag{9}$$

Where the communication coefficient,  $d_i$  is the step size,  $a_{ij}$  can be calculated as

$$\frac{\partial H(u_i[k])}{\partial u_i[k]} = P_{G,i}^{\max} \left( \sum_{i=1}^m u_i[k] P_{G,i}^{\max} - P_D \right). \quad (10)$$

If the communication system for the RG agents is represented using a graph, the communication links between agents are un-directional, i.e.,  $a_{ij}=a_{ji}$ , different methods for  $a_{ji}$  determination provide different converging speeds. Since the mean metropolis algorithm is fully distributed, adaptive to changes of communication network topology, and able to provide convergence guarantee and near optimal converging speed, it is adopted in this paper:

$$a_{ij} = \begin{cases} \frac{2}{(n_i+n_j+1)} & j \in N_i \\ 1 - \sum_{j \in N_i} 2/(n_i + n_j + 1) & i = j \\ 0 & \text{otherwise} \end{cases} \quad (11)$$

Where  $n_i$  and  $n_j$  are the numbers of agents connected to agents  $i$  and  $j$ , respectively,  $N_i$  is the indices of agents that  $P$  communicate with agent  $i$ .

Substituting (10) into (9) yield

$$u_i[k+1] = \sum_{j=1}^m a_{ij} u_j[k] - P_{G,i}^{\max} d_i \left( \sum_{i=1}^m u_i[k] P_{G,i}^{\max} - P_D \right). \quad (12)$$

By defining a  $m$  dimensional communication coefficient matrix  $A$  composed of  $a_{ij}$ s, the overall updating process of the utilization levels in (12) can be represented using matrix form

$$U[k+1] = A \cdot U[k] - \left( \sum_{i=1}^m u_i[k] P_{G,i}^{\max} - P_D \right) \cdot D \quad (13)$$

With

$$U[k] = [u_1[k], \dots, u_i[k], \dots, u_m[k]]^T$$

$$D = [P_{G,1}^{\max} d_1, \dots, P_{G,i}^{\max} d_i, \dots, P_{G,m}^{\max} d_m]^T$$

According to the mean metropolis algorithm, the transition matrix  $A$  is a doubly stochastic matrix, which has the following properties:

- 1) All the eigen values of  $A$  are less or equal to 1
- 2)  $A * v = v, v^T * A = v^T$ , and  $v^T * v = 1$ ,

Where  $v = (1/\sqrt{m})1, 1 = [1, \dots, 1]^T$

According to the Perron- Frobenius theorem, the transition matrix satisfies:  $\lim_{k \rightarrow \infty} A^k = v \cdot v^T = (1/m)1 \cdot 1^T$

As discussed in [22], a distributed subgradient algorithm will converge under two conditions. First, the transition matrix satisfies:  $\lim_{k \rightarrow \infty} A^k = v \cdot v^T = (1/m)1 \cdot 1^T$  will converge under two conditions. Second, the step sizes  $d_i$  s are sufficiently small. Since the designed transition matrix satisfies the first condition automatically and  $d_i$  can be tuned small enough by trial and error for this application, the convergence of the proposed distributed subgradient based generation coordination algorithm can be guaranteed. The equilibrium of the system described by (13) can be obtained by summing up both sides of (12) and letting  $u_i[k+1] = u_i[k] = u_i^*$ , for  $i \in [1, \dots, m]$

$$\sum_{i=1}^m u_i^* = \sum_{i=1}^m \sum_{j=1}^m (a_{ij} u_j^*) - \left( \sum_{i=1}^m u_i^* P_{G,i}^{\max} - P_D \right) \sum_{i=1}^m (P_{G,i}^{\max} d_i). \quad (14)$$

According to (11),  $A$  is a symmetric matrix with the sums of  $\sum_{j=1}^m a_{ji} = 1$ . each equals 1, i.e. .The first term of right hand side of (14) can be calculated as

$$\sum_{i=1}^m \sum_{j=1}^m (a_{ij} u_j^*) = \sum_{i=1}^m \sum_{j=1}^m (a_{ji} u_i^*) = \sum_{i=1}^m \left( u_i^* \sum_{j=1}^m a_{ji} \right) = \sum_{i=1}^m u_i^*. \quad (15)_s$$

ince  $\sum_{i=1}^m P_{G,i}^{\max} d_i \neq 0$ , thus

$$\sum_{i=1}^m u_i^* P_{G,i}^{\max} - P_D = 0. \quad (16)$$

Substituting (16) into (13) with yield  $U[k+1] = U[k] = U^*$

$$U^* = AU^* \quad (17)$$

where  $U^* = [u_1^*, \dots, u_m^*]^T$ .

According to [36], the solution to (17) has the following form:

$$U^* = u^* \cdot \mathbf{1}. \quad (18)$$

By substituting (18) into (16), when the system reaches its steady state, the common utilization level  $u^*$  can be determined

$$u^* = \frac{P_D}{\sum_{i=1}^m P_{G,i}^{\max}} = \frac{P_D}{P_G^{\max}}. \quad (19)$$

Therefore, the proposed control law can achieve the supply-demand balance within the microgrid according to (7).

Measuring the total load and estimating power loss accurately in a distributed way are difficult. Considering the fact that any supply-demand imbalance will be reflected in changes of system frequency, it is intuitive to use frequency deviation to overcome the difficulty.

The following model for dynamic frequency response is proposed in [24]:

$$\frac{df}{dt} = \frac{f_0}{2\omega_{kin0}} \left( \sum_{i=1}^m u_i P_{G,i}^{\max} - P_D \right) \quad (20)$$

Where  $f_0$  is the nominal frequency and  $w_{kino}$  is the initial kinetic energy of the generators, which is decided by the capacity of a power system [24].

Equation (20) can be discretized according to  $df/dt \approx (f[k]-f[k-1])/\Delta t = \Delta f[k]/\Delta t$

$$\Delta f[k] = \frac{f_0 \Delta t}{2\omega_{kin0}} \left( \sum_{i=1}^m u_i[k] P_{G,i}^{\max} - P_D \right) \quad (21)$$

Where  $\Delta t$  is the time step for utilization level update. Therefore

$$\sum_{i=1}^m u_i[k] P_{G,i}^{\max} - P_D = \frac{2\omega_{kin0}}{f_0 \Delta t} \Delta f[k]. \quad (22)$$

By substituting (22) into (12), finally the proposed updating law for the utilization level of RG  $i$  can be represented as

$$u_i[k+1] = \sum_{j=1}^m \alpha_{ij} u_j[k] - \alpha_i \Delta f[k] \quad (23)$$

where  $\alpha_i = 2P_{G,i}^{\max} \omega_{kin0} d_i / f_0 \Delta t$ .

It should be noted that it is unnecessary to estimate  $\omega_{kin0}$  which changes with operating conditions and is hard to accurately estimate. Since its impact on control update has been combined with the other parameters and absorbed into  $\alpha_i$ . Thus, it is preferable and reasonable to tune  $\alpha_i$  directly.

For a specific operating condition  $\alpha_i$  can be identified by trial and error method. Since smaller  $\alpha_i$  usually results in slower convergence, larger  $\alpha_i$  is preferable. However, large  $\alpha_i$  might cause system instability. To achieve a good balance between stability and convergence,  $\alpha_i$  can be initialized with a reasonably small value, such as the 0.1 used for the simulated system. After that, the value of  $\alpha_i$  is kept increasing at a small step size of 0.02 until divergence, which corresponds to stability margin. Half of the that starts to cause instability is selected as the final value. The value of  $\alpha_i$  selected for the simulated system is 0.24.

### 2.3 Algorithm Implementation

The proposed control topology is shown in Fig. 1, which is mainly composed of  $m$  RGs, an SG and  $n$  loads.

Each RG is assigned an RG agent. An RG agent can measure the system's frequency, predict its maximum renewable power generation, and exchange information with its neighboring agents. The supporting communication system for the MAS based solutions can be designed to be independent to the topology of the power network. Even for a complex system, simple communication network can be designed base on cost, location, convenience, etc. Each SG is assigned an SG agent, which does not participate in the utilization level updating process. The SG agent decides the control mode of the SG through control mode selection (CMS), which will be introduced in Section IV

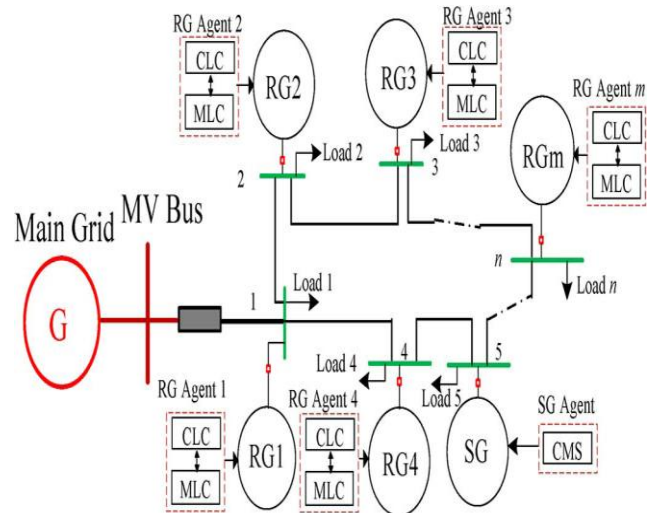


Fig. 1: Illustration of the control topology of a microgrid

The operation of an RG agent is shown in Fig. 2. Each generator agent implements a two-level control strategy. The upper cooperative level control (CLC) discovers the desired utilization level and decides the reference of active power generation. The CLC consists of four function modules. The measurement and prediction module measures the system's frequency and predicts the maximum available renewable generation. The communication module exchanges utilization level information with its neighboring RG agents.

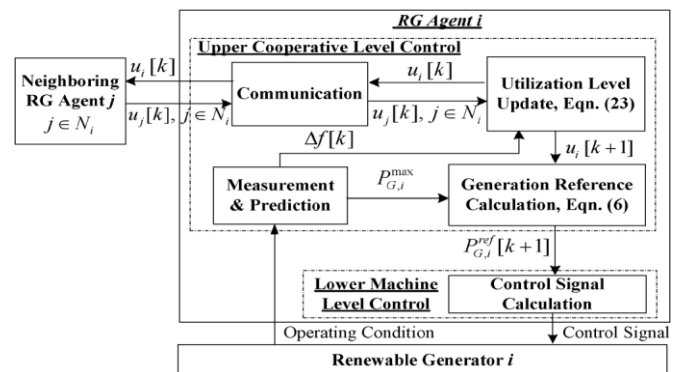


Fig -2: Block diagram of operations of an RG agent.

Based on local frequency deviation Measurements and received utilization levels, the utilization level will be according to (23). The active power generation reference is then calculated based on the utilization level and the predicted maximum renewable power. The lower machine control (MLC) level realizes active power tracking while satisfying other requirements regarding reactive power and terminal voltage regulation. According to the proposed distributed algorithm, there is no need to measure global loading conditions and losses in the

system. Since any supply demand imbalance will result in changes in frequency, the utilization level of an RG can be adjusted based on measured frequency deviation as shown in (23). In this way, the amount of measurements can be significantly reduced. In addition, the complexity and cost of the supporting communication network can also be lowered. The maximum active power generation of a DFIG can be estimated using measured wind speed [37]. In addition, there are many other MPPT algorithms for wind turbine generators available in literature, as summarized in [38]. Similarly, the maximum generation of a PV generator can be predicted based on weather condition (solar insolation, temperature, etc.).

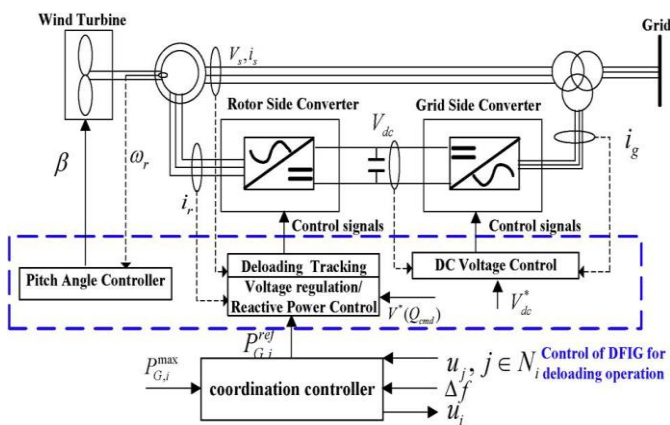


Fig. 3. Machine-level control of DFIG in deloading mode.

A lot MPPT algorithms for PV generators have been developed in the past years [40], such as, fuzzy logic control, neural network, etc. Inaccuracy of the maximum power estimation always exists to some extent due to the prediction errors. Sometimes the predicted value is larger than practical, sometimes smaller. For under-estimation, the predicted generation can be realized. For over-estimation, such as due to the aging problem or internal failures of a PV system, the advantage of the proposed algorithm will present. The proposed algorithm updates generation references based on overall generation estimations and overall demand. Since the generation reference settings are usually lower than the under sufficient renewable generation, the impact of inaccurate estimation can be lowered.

#### IV. CONTROL OF DIFFERENT TYPES OF DGS:

##### A. Control of DFIG:

The machine-level control of each DFIG manages active power reference tracking, as well as reactive power or terminal voltage regulation and DC-link voltage regulation. As illustrated in Fig. 3, the machine-level control consists of the electrical control of two converters and the mechanical control of pitch angle. A typical DFIG model introduced in [42] is adopted in this paper. The active power generation of the DFIG can be regulated by controlling rotor speed and/or tuning pitch angle. The former method is preferred for two reasons. First, is controlled by converter control, whose response speed is faster than the mechanical pitch angle control. Second, electrical control of can decrease wear and tear on the pitch blade. However, when the rotor speed reaches the upper bound, it is necessary to activate the pitch angle tuning. The implementation details of DFIG control are presented.

##### 1) Converter Control:

In this paper, the DFIG is controlled by back-to-back converters. With the decoupled control method; the rotor-side converter (RSC) controls both the active and reactive power of the DFIG. The active power is controlled by adjusting the -axis rotor current, while the reactive power is controlled by adjusting the -axis rotor current, as shown in Fig. 4. The deviation between the active power output of DFIG and the reference value forms the error signal that is processed by a PI controller to produce the rotor current reference. Through another PI controller, the difference

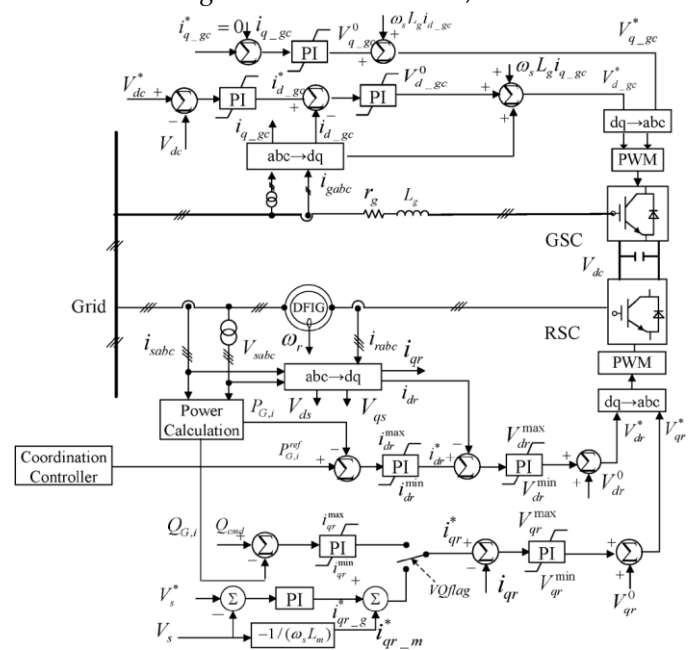


Fig. 4. Schematic diagram of control strategy for RSC and GSC of a DFIG.

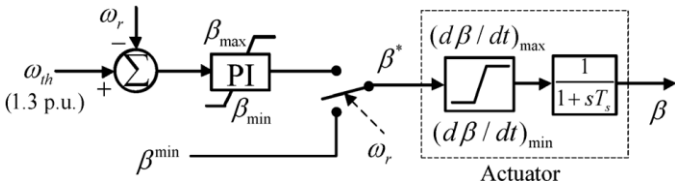


Fig. 5. Pitch angle control system.

Between rotor current and reference value is used to produce rotor voltage. There are two modes for reactive power control, the voltage and reactive power regulation modes. Both modes regulate q-axis rotor current. In voltage regulation mode, is controlled to reduce voltage fluctuation. For reactive power regulation, the difference between the reactive command and the reactive power output forms rotor current reference through a PI controller. Here, GSC is used only to stabilize the DC-link voltage.

**Pitch Angle Control:**

The pitch angle control method, as depicted in Fig. 5, consists of a PI controller and a pitch angle actuator. The threshold speed is set to 1.3 p.u., and is set to 0. The maximum pitch angle change rate

**PV Control**

The PV system model described in [47] is adopted in this paper. and are the solar array voltage and current, respectively, and are the local bus voltage and current. In this paper, PV is controlled in unit power factor mode. If a PV system is equipped with in isolation and temperature sensors, the following method introduced in can be used to estimate the maximum generation of :

$$P_{G,i}^{max} = P_{STC} \frac{G_{ING}}{G_{STC}} [1 + k_{pv}(T_c - T_r)] \quad (24)$$

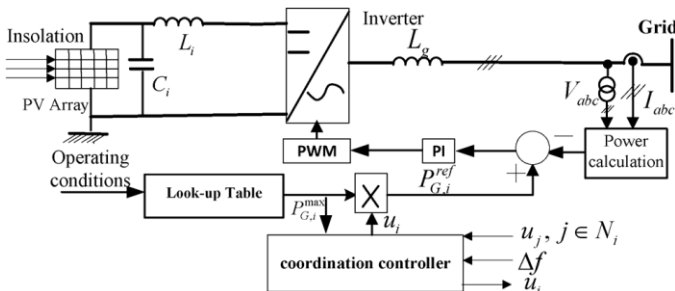


Fig. 6. Control strategy for PV system.

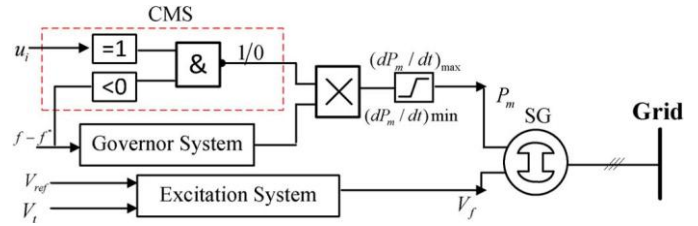


Fig. 7. Control logic of synchronous machine.

Where  $P_{STC}$  is the module maximum power at standard test condition (STC),  $G_{ING}$  is the incident irradiance, is irradiance at STC  $1000(W/m^2)$ ,  $K_{PV}$  is the temperature coefficient of power, and  $T_c$  and  $T_r$  are the cell temperature and the reference temperature (25 ), respectively. Once  $P_{G,i}^{max}$  and  $u_i$  have been calculated, the generation reference  $P_{G,i}^{ref}$  can be updated according to (6). After that, simple PI control can be used to control the inverters for active power tracking, as shown in Fig. 6.

**Control of SG**

In this paper, the SG in the renewable micro grid has two functions. If the renewable generation is sufficient to power all loads, SG is just used for voltage regulation. If the renewable generation is insufficient, in addition to voltage regulation, the SG also generates active power to compensate the deficiency. The SG does not need to participate in the discovery of desired utilization level. The SG agent can monitor the instantaneous utilization level of one of its nearby RGs in order to determine its control mode through CMS, as shown in Fig. 7. If the utilization level equals to 1 and the frequency deviation is negative, the SG will generate active power to compensate the deficiency of the renewable generation. Otherwise, the SG will only provide reactive power support to maintain local voltage level. A rate limiter is used to model the ramp rate of the SG in the control loop. The governor system is modeled as a PI controller. The excitation system block adopts a DC exciter.

**V. SIMULATION STUDIES:**

The proposed fully-distributed cooperative control algorithm is tested with a 6-bus micro grid model using MATLAB/SIMULINK, as shown in Fig. 8. The system contains six loads, three DFIGs, two PVs and one SG. The DFIG at bus-1 (abbreviated as DFIG-1) is controlled in reactive power regulation mode, the DFIG-4 and DFIG-5 are controlled in voltage regulation mode, and the PV-2 and PV-3 are controlled in unit power factor mode, as

introduced in Section IV. The ramp-up and ramp-down rates of the SG are both set to 0.4 MW/s

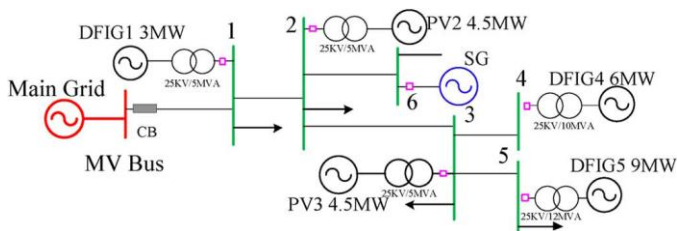


Fig. 8. Configuration of a 6-bus microgrid.

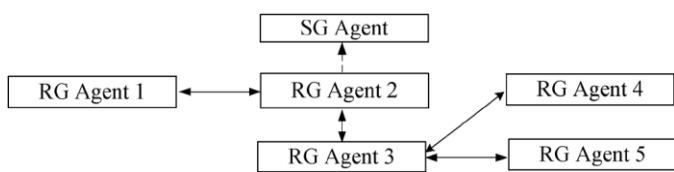


Fig. 9. Communication topology of the MAS for 6-bus micro grid

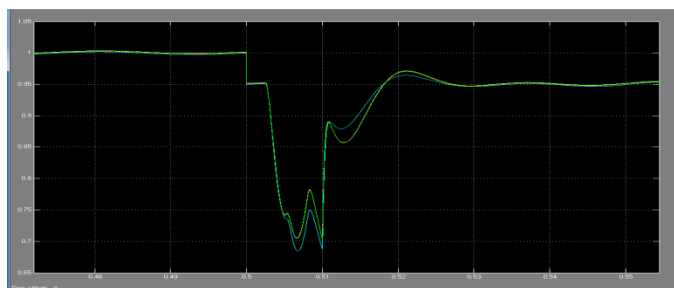


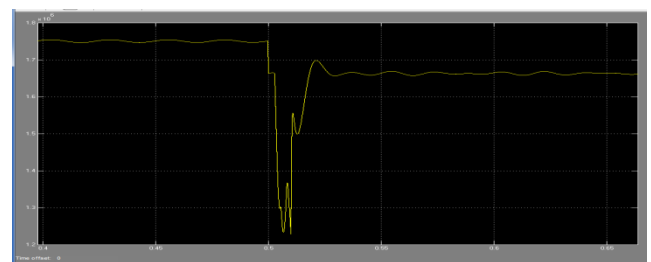
Fig. 10. Utilization level profiles of 5 RGs (Test 1).

The communication topology of the MAS for the 6-bus micro grid is as shown in Fig. 9. During simulations, time step for utilization level update is selected to be 0.1 s, which has good balance of control performance and technical feasibility. The proposed control strategy is tested under two operating conditions. Test 1 establishes a constant available renewable generation and loads. Test 2 has a variable available renewable generation and loads. The first test is unrealistic yet easier to understand due to its simplicity.

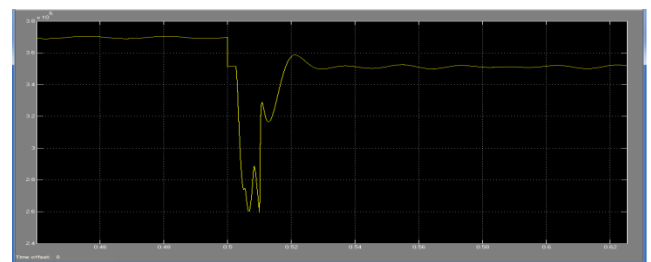
**Test 1**

In the first test, the demands of the loads remain constant. The wind speeds of the DFIGs at bus-1, bus-4, and bus-5 are constant at 11 m/s, 14 m/s, and 14 m/s, respectively. The solar insolation of PVs at bus-2 and bus-3 are 900 and 1000 , respectively. An islanding event at 0.2 s is simulated

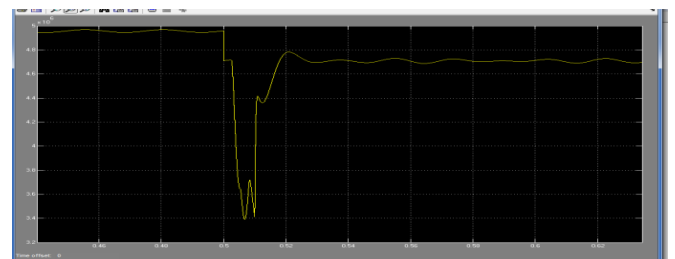
to test the performance of the proposed control strategy. Fig. 10 shows the utilization level profile. Before islanding, RGs are controlled using the MPPT algorithm, and the initial output of the SG is set to 2 MW to create enough disturbances to test the performance of the proposed control algorithm. At the instant of islanding, the available renewable power is more than the load demand, the system’s frequency increases at this moment as shown in Fig. 12.



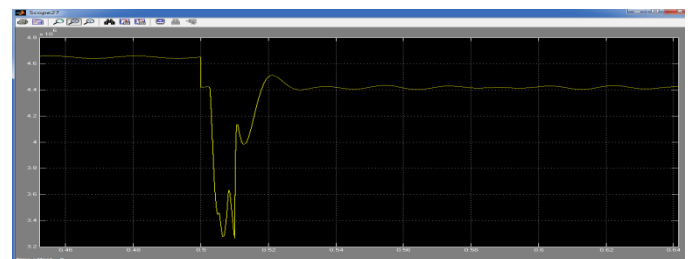
(a)



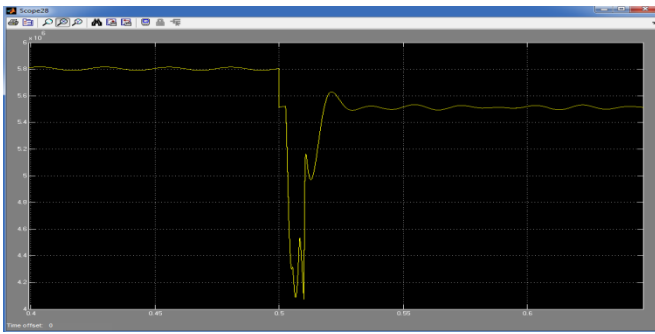
(b)



(c)

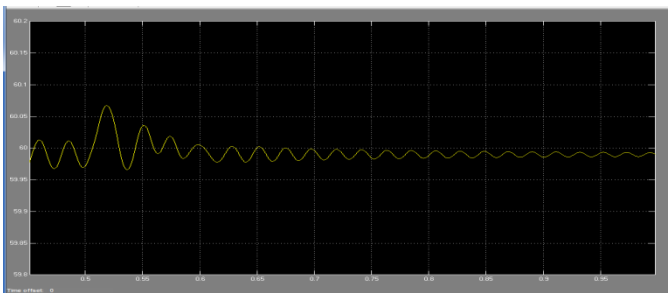


(d)

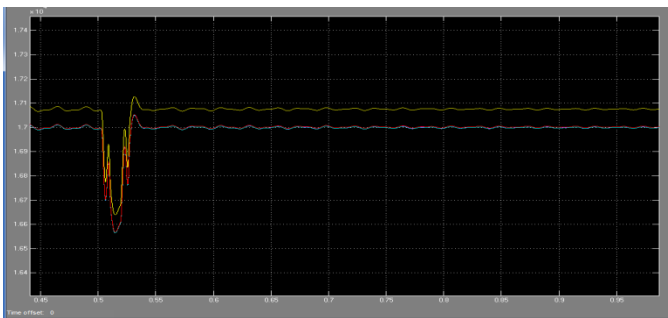


(e)

**Fig. 11. Dynamic response of DGs. (a) DFIG-1 active power output; (b) PV-2 active power output; (c) PV-3 active power output; (d) DFIG-4 active power output; (e) DFIG-5 active power output.]**



(a)

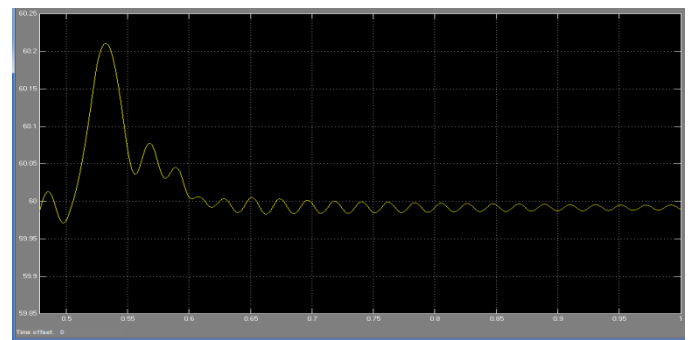


(b)

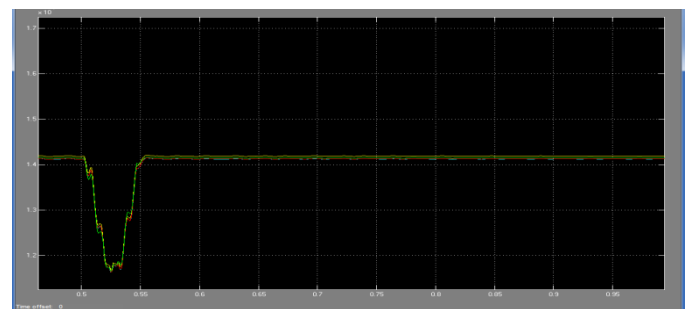
**Fig. 12. System response under the proposed solution. (a) Frequency response; (b) terminal voltages of DGs.**

Fig. 11 shows the dynamic responses of the DGs. The active power generations of the DGs converge to a value below the maximum available power after islanding. The utilization levels, if calculated, are the same as the ratio of actual output power to MPPT power. To evaluate the performance of the proposed algorithm, the traditional Droop-AGC method is simulated for comparison. Droop

control is used to adjust the generations based on predefined P-f Q-V characteristic. AGC is applied every 5 s to eliminate frequency deviation. The dynamic responses under the proposed algorithm and Droop-AGC method are shown in Figs. 12 and 13, respectively. By comparing Figs. 12(a) and 13(a), one can see that the frequency response under the proposed solution is able to converge to the nominal value within less time, while it takes more time in the Droop-AGC method. In addition, the overshoot of frequency response under the proposed algorithm is much smaller than that of the conventional droop method. Similar observations can be made for voltage responses under the proposed algorithm and Droop-AGC method, as shown in Figs. 12(b) and 13(b), respectively. The improved performance comes from dynamic and accurate generation adjustments as compared to using fixed P-f and Q-V characteristics.



(a)



(b)

**Fig. 13. System response under the Droop-AGC method. (a) Frequency response; (b) terminal voltages of DGs.**

Based on the simulation results, it can be concluded that the algorithm proposed in the paper can also be applied to coordinate multiple SGs in a traditional power system and the performance will be better than that of traditional Droop-AGC controls. However, because of the intermittency and unreliability of renewable energy

resources, the maximum generations of RGs are usually time-varying. To achieve accurate power sharing, the droop control parameters, and , need to be adjusted dynamically based on instantaneous operating conditions, which is hard to realize. In addition, even if the periodical AGC can be applied much faster than current practice of 10 s or longer such as the 5 s adopted in simulation, it still might be insufficient for autonomous renewable micro grid that has reduced inertia. Thus, Droop-AGC is not simulated in the following test under variable renewable generation.

### B. Test 2

As shown in Fig. 14, the proposed algorithm is good at coordinating the utilization level of five RGs to a common value. The utilization level drops below 1 immediately after grid disconnection. The SG switches to voltage regulation mode and its active power generation gradually decreases from 4MW to zero

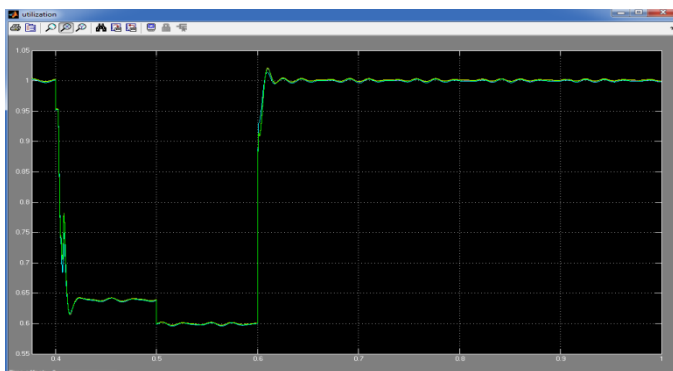


Fig. 14. Utilization level profiles of 5 RGs (Test 2).

according to the pre-defined ramp-down rate. At 0.5 s, a load of 2 MW is shed, and the utilization level drops so that the RGs can reduce the renewable generation. The utilization level rises at 0.6 s when the load is restored. When the estimated maximum renewable generation is insufficient, the utilization level reaches the upper bound and is capped at 1, and all of the RGs are controlled in MPPT mode, which can be observed during the period from 0.4 s to 1 s. Meanwhile, the SG is controlled to generate active power to compensate for the deficiency, as shown in Fig. . To illustrate the dynamic performance of the utilization level, the available total renewable generation and total load profiles are plotted together in Fig. When the loads are modeled as serial RLC modules with constant parameters, the actual load will oscillate due to frequency and voltage fluctuations. This phenomenon

can be observed when operating conditions change in Fig.. Investigating the responses of the frequency and terminal voltages (Fig.17) helps to clarify this phenomenon. The actual active power generation, and the available maximum wind power of DFIG-4. DFIG-4 (0.4sto0.5 s). Similar performances can be observed for other RGs, which are not shown here. Fig.16 shows the active and reactive power generation of the SG. At the instant of islanding at 0.4 s, the active power generation of the SG is gradually reduced to 0 because the available renewable generation is more than the total load demand.

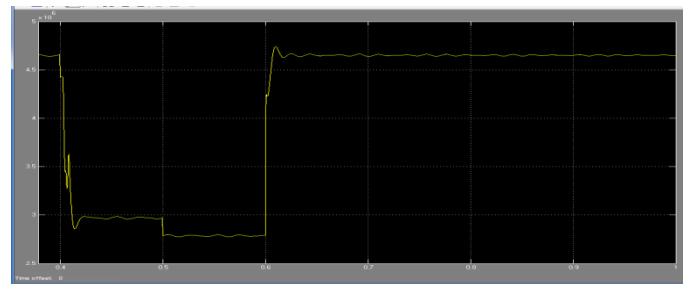


Fig. 15. Active power tracking of DFIG-4

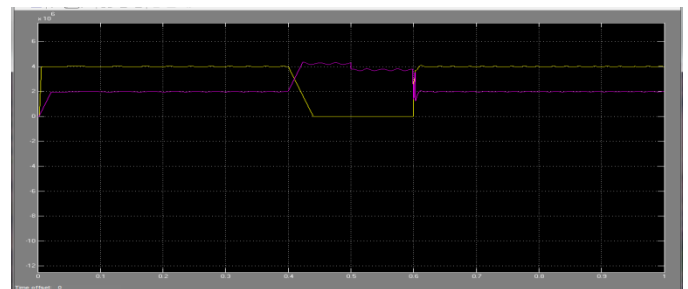
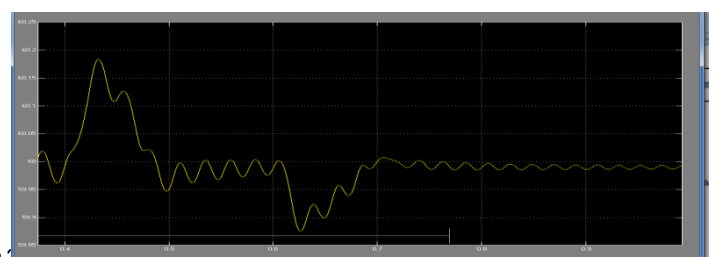
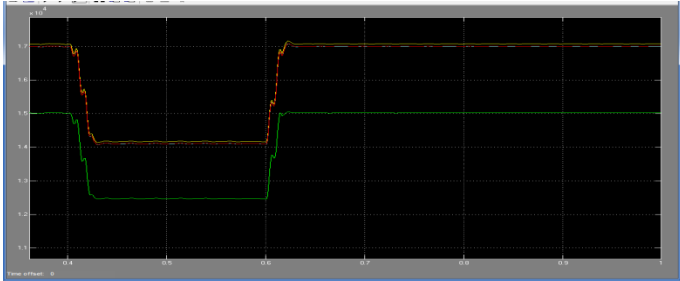


Fig. 16. Active and reactive power of the SG.

The decreasing slope of active power generation is decided by the ramp rates of the SG. When there is insufficient renewable generation ( and frequency deviation is negative), the SG is controlled to generate active power to compensate for insufficient power during 0.5s to 1s. The frequency and voltage responses are usually customers' main concerns, and they should be evaluated by up-to-date standards and regulation codes. According to the IEEE Std. 1547 [53], the normal frequency should be within the range of 59.8 Hz–60.5



(a)



(b)

**Fig.17. System response of test 2. (a) System frequency response; (b) terminal voltages of DGs.**

## VI. CONCLUSION:

This paper targets at the coordination problem with an autonomous micro grid under high penetration of renewable energy. Two main reasons motivate the authors to control the utilization level to a common value instead of controlling some RGs in MPPT mode and others in reduced generation mode. First, MPPT algorithms that emphasize high renewable energy utilization may cause supply-demand imbalance when the available renewable generation is more than demanded. Second, every MPPT algorithm has the problem of impreciseness to certain degree and the predicted maximum available generation might be unachievable. By synchronizing the utilization levels of the RGs to a common value, the impacts of prediction impreciseness of the MPPT algorithms can be efficiently mitigated. The proposed control scheme has the following four main advantages. The first advantage is the introduction of a simple MAS-based fully distributed method. Due to the simplicity of the network topology and the reduced amount of information to exchange, the cost of the supporting communication network will be much lower than that of a centralized solution. The second is its avoidance of the direct measurements of loading conditions. The third is its distributed coordination of different types of DGs (DFIG, PV, and SG), which can maintain the supply-demand balance within the micro grid. The fourth is its introduction of the sub gradient optimization method, which improves the system's dynamic performance. Simulation studies demonstrate

that the multiple RGs and the SG are well coordinated to maintain the power supply-demand balance for the autonomous micro grid in both excessive and insufficient available renewable power situations.

## REFERENCES

- [1] Distributed Subgradient-Based Coordination of Multiple Renewable Generators in a Microgrid IEEE
- [2] A.Mehrizi-Sani, A. H. Etemadi, D. E. Olivares, and R. Iravani, "Trends in microgrid control," *IEEE Trans. Smart Grid*, to be published
- [3] N. Femia, G. Petrone, G. Spagnuolo, and M. Vitelli, "Optimization of perturb and observe maximum power point tracking method," *IEEE Trans. Power Electron.*, vol. 20, no. 4, pp. 963–973, 2005.
- [4] E. Koutroulis and K. Kalaitzakis, "Design of a maximum power tracking system for wind-energy-conversion applications," *IEEE Trans. Ind. Electron.*, vol. 53, no. 2, pp. 486–494, 2006.
- [5] L. Qu and W. Qiao, "Constant power control of DFIG wind turbines with supercapacitor energy storage," *IEEE Trans. Ind. Applicat.*, vol. 47, no. 1, pp. 359–367, 2011.
- [6] J. L. Rodriguez-Amenedo, S. Arnalte, and J. C. Burgos, "Automatic generation control of a wind farm with variable speed wind turbines," *IEEE Trans. Energy Convers.*, vol. 17, no. 2, pp. 279–284, 2002.
- [7] R. G. de Almeida, E. D. Castronuovo, and J. A. P. Lopes, "Optimum generation control in wind parks when carrying out system operator requests," *IEEE Trans. Power Syst.*, vol. 21, no. 2, pp. 718–725, May 2006.
- [8] L. R. Chang-Chien, C. M. Hung, and Y. C. Yin, "Dynamic reserve allocation for system contingency by DFIG wind farms," *IEEE Trans. Power Syst.*, vol. 23, no. 2, pp. 729–736, May 2008.
- [9] T. Senjyu, A. Yona, M. Datta, H. Sekine, and T. Funabashi, "A coordinated control method for leveling output power fluctuations of multiple PV systems," in *Proc. Int. Conf. Power Electronics*, 2007, pp. 445–450.
- [10] H. Xin, Z. Qu, J. Seuss, and A. Maknouninejad, "A self-organizing strategy for power flow control of photovoltaic generators in a distribution network," *IEEE Trans. Power Syst.*, vol. 26, no. 3, pp. 1462–1473, Aug. 2011.
- [11] A. Dimeas and N. Hatziargyriou, "A multiagent system for microgrids," in *Proc. IEEE Power Engineering Society General Meeting*, 2004, vol. 1, pp. 55–58.

[12] C. M. Colson and M. H. Nehrir, "Algorithms for distributed decisionmaking for multi-agent microgrid power management," in *Proc. 2011 IEEE Power and Energy Society General Meeting*, 2011, pp. 1–8.

[13] B. Zhao, C. X. Guo, and Y. J. Cao, "A multiagent-based particle swarm optimization approach for optimal reactive power dispatch," *IEEE Trans. Power Syst.*, vol. 20, no. 2, pp. 1070–1078, May 2005.

[14] A. L. Kulasekera, R. A. R. C. Gopura, K. T. M. U. Hemapala, and N. Perera, "A review on multi-agent systems in microgrid applications," in *Proc. 2011 IEEE PES Innovative Smart Grid Technologies*, 2011, pp. 173–177.

[15] Y. Xu and W. Liu, "Novel multi agent based load restoration algorithm for microgrids," *IEEE Trans. Smart Grid*, vol. 2, no. 1, pp. 140–149, 2011.

[16] Y. Xu, W. Liu, and J. Gong, "Multi-agent based load shedding algorithm for power systems," *IEEE Trans. Power Syst.*, vol. 26, no. 4, pp. 2006–2014, Nov. 2011

[17] W. Zhang, Y. Xu, W. Liu, F. Ferrese, and L. Liu, "Fully distributed coordination of multiple DFIGs in a microgrid for load sharing," *IEEE Trans. Smart Grid*, to be published

## BIOGRAPHIES

**V.SRINIVASULU** has received B.Tech degree in electrical and electronics engineering from GPREC KURNOOL, AP



under SRIKRISHNADEVARAYA University. Presently he is doing Post graduation in Electrical power systems Specialization at J.N.T.U.A, Anantapur. His main areas of interest include power systems, FACTS, Renewable energy resources, microgrid

**M MADHUSUDHAN REDDY** received B.Tech degree in



electrical & electronics engineering from KTMC, AP. He did Post graduation in power electronics & drives Specialization. Presently working as a Head of the EEE department